

DOE Award No.: DE-FE0028973

Quarterly Research Performance Progress Report

(Period Ending 9/30/2018)

Advanced Simulation and Experiments of Strongly Coupled Geomechanics and Flow for Gas Hydrate Deposits: Validation and Field Application

Project Period (10/01/2016 to 09/30/2019)

Submitted by:
Jihoon Kim



Signature

The Harold Vance Department of Petroleum Engineering,
College of Engineering
Texas A&M University
501L Richardson Building
3116 College Station TX, 77843-3136
Email: jihoon.kim@tamu.edu
Phone number: (979) 845-2205

Prepared for:
United States Department of Energy
National Energy Technology Laboratory

September 30, 2018



U.S. DEPARTMENT OF
ENERGY

**NATIONAL ENERGY
TECHNOLOGY LABORATORY**

Office of Fossil Energy

DISCLAIMER

This report was prepared as an account of work sponsored by an agency of the United States Government. Neither the United States Government nor any agency thereof, nor any of their employees, makes any warranty, express or implied, or assumes any legal liability or responsibility for the accuracy, completeness, or usefulness of any information, apparatus, product, or process disclosed, or represents that its use would not infringe privately owned rights. Reference herein to any specific commercial product, process, or service by trade name, trademark, manufacturer, or otherwise does not necessarily constitute or imply its endorsement, recommendation, or favoring by the United States Government or any agency thereof. The views and opinions of authors expressed herein do not necessarily state or reflect those of the United States Government or any agency thereof.

TABLE OF CONTENTS

	<u>Page</u>
DISCLAIMER	2
TABLE OF CONTENTS	3
ACCOMPLISHMENTS	4
Objectives of the project.....	4
Accomplished	4
Task 1	4
Task 2	5
Task 3	7
Task 4	11
Task 5	13
Task 6	16
PRODUCTS	16
BUDGETARY INFORMATION.....	16

ACCOMPLISHMENTS

Objectives of the project

The objectives of the proposed research are (1) to investigate geomechanical responses induced by depressurization experimentally and numerically; (2) to enhance the current numerical simulation technology in order to simulate complex physically coupled processes by depressurization and (3) to perform in-depth numerical analyses of two selected potential production test sites: one based on the deposits observed at the Ulleung basin UBGH2-6 site; and the other based on well-characterized accumulations from the westend Prudhoe Bay. To these ends, the recipient will have the following specific objectives:

1). Information obtained from multi-scale experiments previously conducted at the recipient's research partner (the Korean Institute of Geoscience and Mineral Resources (KIGAM)) that were designed to represent the most promising known Ulleung Basin gas hydrate deposit as drilled at site UBGH2-6 will be evaluated (Task 2). These findings will be further tested by new experimental studies at Lawrence Berkeley National Laboratory (LBNL) and Texas A&M (TAMU) (Task 3) that are designed capture complex coupled physical processes between flow and geomechanics, such as sand production, capillarity, and formation of secondary hydrates. The findings of Tasks 2 and 3 will be used to further improve numerical codes.

2) Develop (in Tasks 4 through 6) an advanced coupled geomechanics and non-isothermal flow simulator (T+M^{AM}) to account for large deformation and strong capillarity. This new code will be validated using data from the literature, from previous work by the project team, and with the results of the proposed experimental studies. The developed simulator will be applied to both Ulleung Basin and Prudhoe Bay sites, effectively addressing complex geomechanical and petrophysical changes induced by depressurization (e.g., frost-heave, strong capillarity, cryo-suction, induced fracturing, and dynamic permeability).

Accomplished

The plan of the project timeline and tasks is shown in Table 1, and the activities and achievements during this period are listed as follows along with Table 2.

Task 1: Project management and planning

The seventh quarterly report was submitted to NETL on July 30, 2018. The Budget Period 2 to 3 transition meeting with TAMU, LBNL, KIGAM, NETL was held at July 26, 2018. LBNL has completed Subtask 3.2 and been actively working on Subtask 3.3. TAMU has completed Subtask 3.5, and is initiating Subtask 3.4. TAMU and KIGAM are working on Subtasks 4.1 and 5.2 related to the experiment of Task 2, validation of T+M with the experimental data. TAMU has been working on Subtask 5.3 and 5.4 for the modeling of plastic behavior and induced fracturing. Also, TAMU, KIGAM, and LBNL are actively working on Subtasks 4.2, 4.3, 5.5, and 5.6. The specific status of

the milestones is shown in Table 2. Specific achievements including publication during this period are as follows.

Task 2: Review and evaluation of experimental data of gas hydrate at various scales for gas production of Ulleung Basin

Subtask 2.1 Evaluation of Gas hydrate depressurization experiment of 1-m scale

This task was completed previously.

Subtask 2.2 Evaluation of Gas hydrate depressurization experiment of 10-m scale

This task was completed previously.

Subtask 2.3 Evaluation of Gas hydrate depressurization experiment of 1.5-m scale system in 3D

This task was completed previously. Here, we further describe the experimental results, which are closely related to Subtask 4.1, focusing on depressurization experiment after gas hydrate formation.

The initial temperature and pressure was 15.2°C and 20.1 MPa, respectively. The depressurization test was conducted in three stages. The range of the first stage was from 20.1MPa to 10.1MPa, the range of the second stage was from 10.1MPa to 7.6MPa, and the depressurization rate was -0.42MPa/h in both stages. The last stage was to reduce the pressure to atmospheric pressure, which is the step for mass balance calculation, not dissociation.

Fig. 2.3.1, 2.3.2, Fig.2.3.3 show the pressure change, water production and total gas production of the high-pressure cell during the depressurization test, respectively. In Fig. 2.3.1, the pressure responses measured at the edge (50 cm from the center) and inside (5 cm from the center) of the sediment were almost similar, and the pressure at each height of the sediment layer was similar, although not shown here. The total amount of water produced during the first, second and the third depressurization are about 190 L, 28L, and 16L, respectively. Most of the water was produced during the first depressurization in which the gas hydrate dissociation started, and the water production during the second depressurization after completion of the dissociation was only 18% of the total production. This can be explained as follows. The pores of sediment sample are initially saturated with water and gas hydrates. When the dissociation starts, water is preferentially produced by the dissociated gas from hydrates in the pores. Water production is significantly reduced after completion of the dissociation, because the majority of the pores is saturated with the gas phase.

Total gas production at the first stage begins to increase at the beginning of depressurization, but the gas production is the amount of dissolved gas that escapes from the produced water in atmospheric pressure, not the amount dissociated from hydrates in the sediment. The gas production from hydrate dissociation is delayed after the first stage. Gas production at the second stage includes dissolved gas and free gas, but mainly due to the gas dissociated from the first depressurization. The total amount of gas produced during the first, second and the third depressurization are about 2,328 L, 11,426L, and 35,790L, respectively.

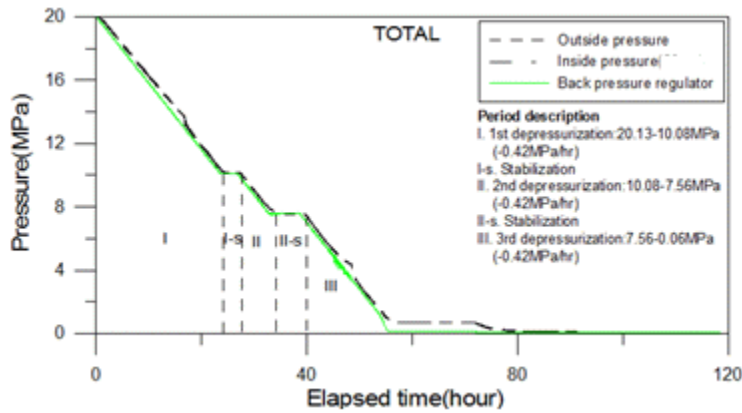


Fig.2.3.1 Sediment pressure and back pressure during the depressurization test

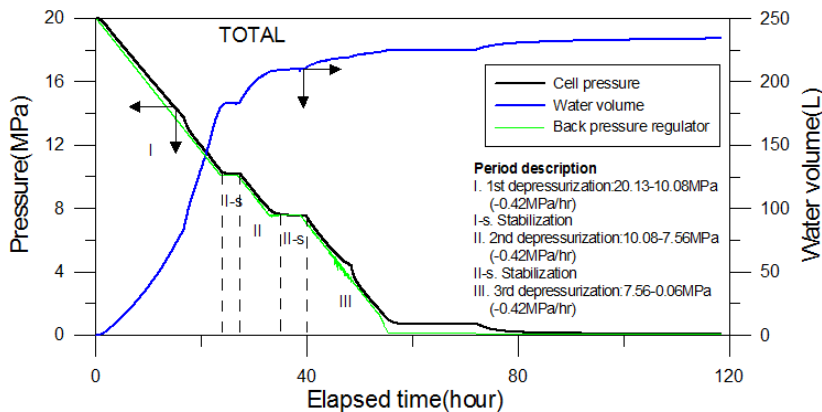


Fig. 2.3.2 Total water production during the depressurization test

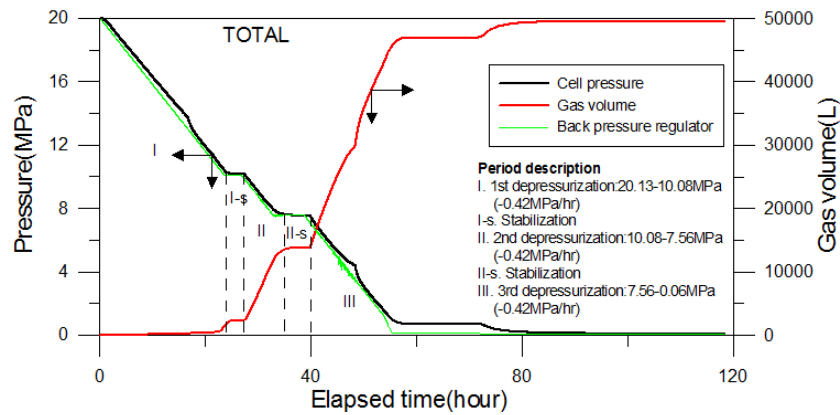


Fig. 2.3.3 Total gas production during the depressurization test

Subtask 2.4 Evaluation of gas hydrate production experiment of the centimeter-scale system

This task was completed previously.

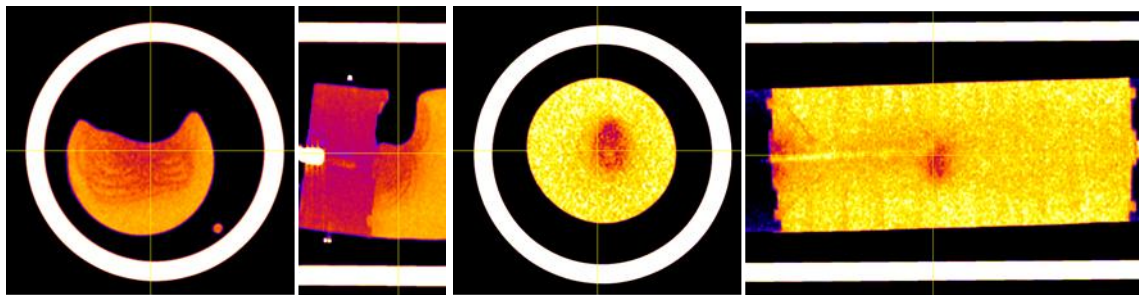
Task 3: Laboratory Experiments for Numerical Model Verification

Subtask 3.1: Geomechanical changes from effective stress changes during dissociation

This task was completed, previously.

Subtask 3.2 Geomechanical changes from effective stress changes during dissociation – sand

This task was completed. Along with the previous description, we performed the experiment to investigate geomechanical changes when the effective stress was increased to 300psi. The flow rate is 2 mL/min. The majority of the sand movement shown in Fig. 3.2.1 occurs during flow, not confining pressure changes. More experimental analysis is ongoing with Task 4.



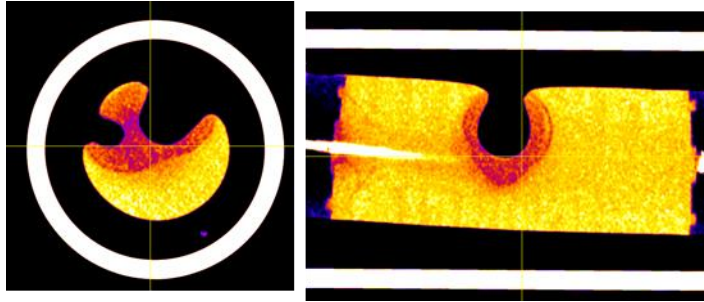


Fig. 3.2.1 X-ray CT images of the sample at the flow rate of 2mL/min

Subtask 3.3 Geomechanical changes resulting from secondary hydrate and capillary pressure changes

We are initiating the experiment of this task, the schematics of which is shown in Fig. 3.2.2. We designed and built a number of capillary pressure “stones” working with SoilMoisture Equipment (Fig. 3.2.2). These will be saturated and filled with water, and connected to the low pressure end of a differential pressure transducer. The stones were manufactured using three different types of ceramics, having nominal gas entry pressures of 1 bar, 5 bars, and 15 bars.

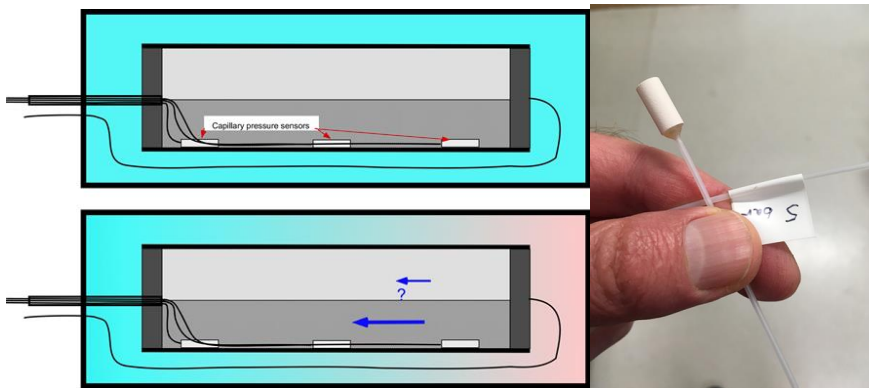


Fig. 3.2.2 Experimental schematics and equipment.

Subtask 3.4 Construction of the Relative Permeability Data in Presence of Hydrate

Not initiated (future year tasks)

Subtask 3.5 Identification of Hysteresis in Hydrate Stability

This subtask is completed. Here we add more descriptions of the findings in this experiment. For the information of the experimental setting, the readers can refer to the previous quarterly reports.

The curve in Fig. 3.5.1 shows the phase equilibrium curve, and the blue dots represent an experimental value for a pressure and temperature. The difference in pressure from the experimental and the equilibrium line was either positive, which means that the system can form hydrates, or negative, meaning that under equilibrium conditions there was no hydrate formation. Fig. 3.5.2 shows $\Delta P (=P_{exp} - P_{eq})$ on the left, and the thermal difference on the right. Clearly, the thermal gradient shows some variance but is very close for cycles 1, 3, 4, and 5. Table 3.5.1 shows hysteresis of hydrate formation. From the table, we can find existence a clear pattern and a correlation to the maximum temperature and the formation time. Fig. 3.5.3 shows pressure response to thermal spikes, showing the strong correlation between the temperature peaks and the hydrate consumption. The yellow line shows clearly that there is consumption of methane at the temperature spikes.

Fig. 3.5.4 shows the normalized initial formation time for the different melting temperatures for Cycles 3, 4, and 5. The equation in the figure for the delta time shows a clear trend of the melting temperature on the system, while the equation is simple. This also shows the higher the melting temperature the closer the system behavior to the first cycle in the absence of hysteresis.

In summary, from this experiment, hysteresis has been observed in both initial formation times and at the temperature spike times. A simple predictive model has been developed.

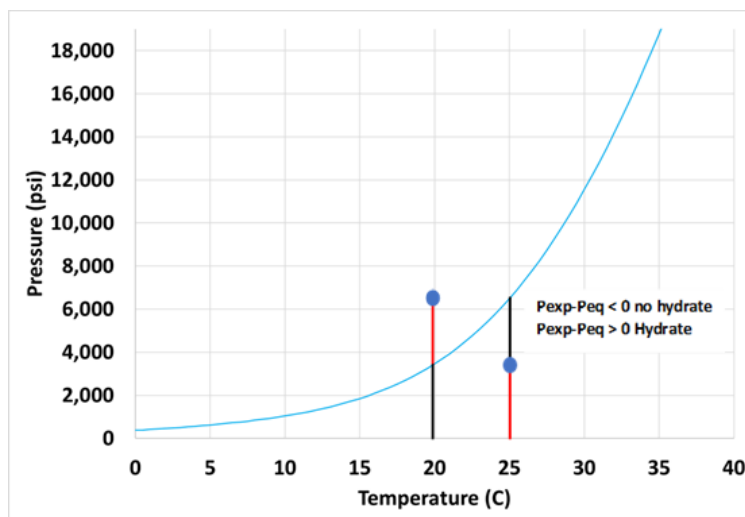


Fig. 3.5.1 Phase diagram for Methane Hydrate with distance idea

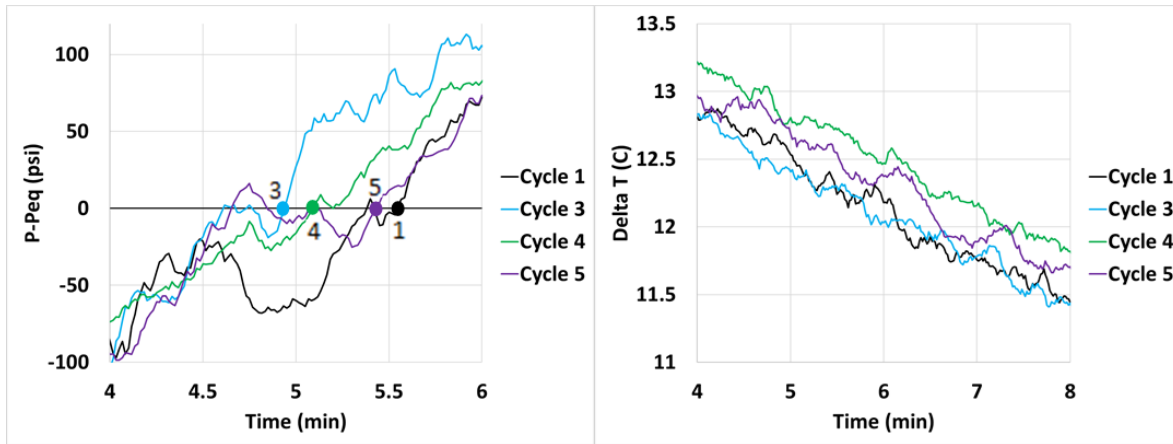


Fig. 3.5.2 Close-up of the ΔP Near Zero.

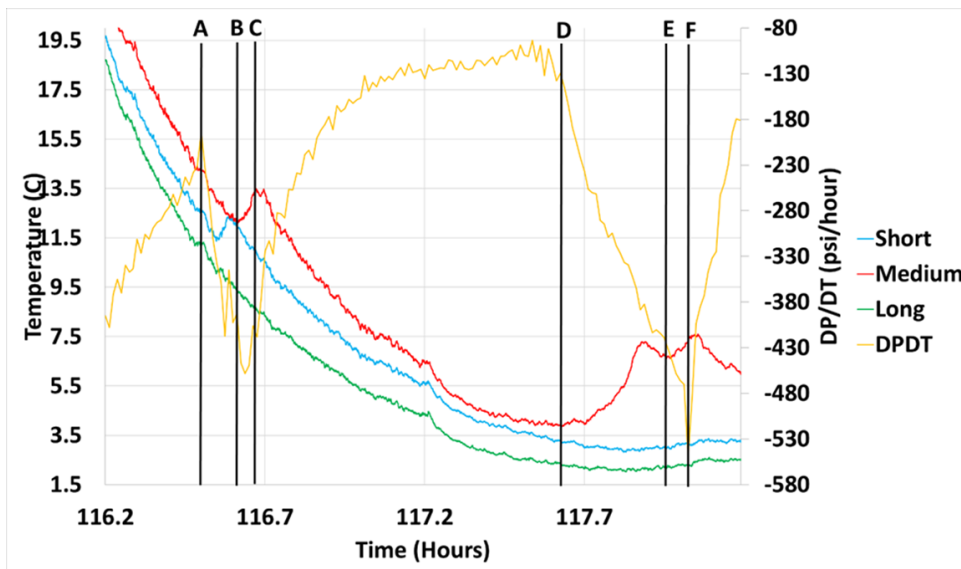


Fig. 3.5.3 Pressure response to thermal spikes

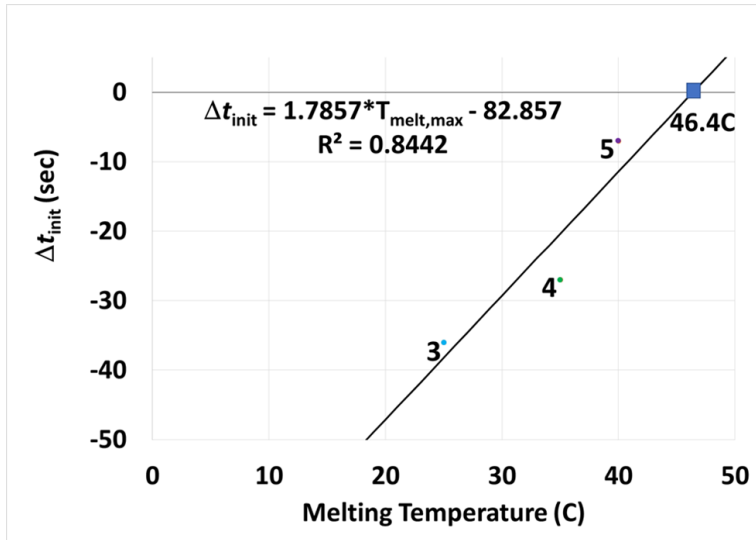


Fig. 3.5.4 Normalized initial formation time versus melting temperature for Cycles 3, 4, and 5.

Table 3.5.1: Recorded maximum temperature and hydrate formation time for the cycles 1-5

Cycle	1	3	4	5
Max Temp (C)	25	25	35	40
Formation time (s)	332	296	305	325

Task 4: Incorporation of Laboratory Data into Numerical Simulation Model

Subtask 4.1 Inputs and Preliminary Scoping Calculations

Continuing the previous work, we have been post-processing the data from Subtasks 2.2 and 2.3. We have also been reviewing the data of Subtask 2.1, again, correcting the information and input data for simulation of Subtask 5.2.

Subtask 4.2 Determination of New Constitutive Relationships

Continuing the work in the previous quarter, we have still been modifying the subroutines of the hysteretic capillarity and relative permeability during this quarter. Also, from Subtask 3.5, we have also proposed the equation shown in Fig. 3.5.4

Subtask 4.3 Development of Geological Model

We have constructed the geological model based on the axisymmetric domain for Site UBGH2-6 in the Ulleung Basin first to perform numerical simulation as shown in Subtask 5.5. Specifically, the site of UBGH2-6 is located in South Korea, having significant overburden in the deep sea (Fig. 4.3.1). The methane hydrate zone consists of alternating hydrate-bearing sand and mud layers. For numerical simulation, we take the domain of 250m by 220m, which has irregular sizes of grid blocks (160 by 140).

Gas is produced by depressurization with the constant bottom hole pressure of 9MPa. Table 4.3.1 presents major properties of flow and geomechanics simulation. The initial pressures at the top and bottom are 23.1MPa and 24.59MPa, respectively, and the initial temperatures at the top and bottom are 6.366 °C and 18.633 °C, respectively. They are distributed linearly from top to bottom. The initial hydrate saturation at the hydrate zone is 0.65, while it is zero at the other zones. The initial vertical and horizontal stresses are -23.1MPa and -3.47 MPa, respectively, and they are distributed vertically with the gradients of -25.0kPa and -3.47 kPa. Tensile stress is positive.

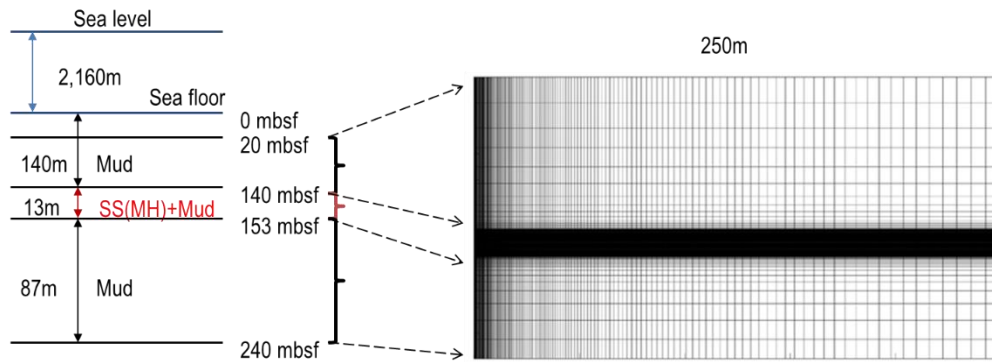


Fig. 4.3.1 Left: geological information of UBGH2-6 Right: discretized domain for flow

Table 4.3.1. Material properties for flow and geomechanics

Property	Overburden	Hydrate layer	Mud-Interlayer	Underburden
Drained bulk modulus, SH=0%	15.55 MPa	27 MPa	20 MPa	22 MPa
Drained shear modulus, SH=0%	5.185 MPa	16 MPa	6.667 MPa	7.407 MPa
Drained bulk modulus, SH=100%	285 MPa	933.33 MPa	285 MPa	285 MPa
Drained shear modulus, SH=100%	99.75 MPa	560 MPa	99.75 MPa	99.75 MPa
Permeability, SH=0%	0.02 mD	500 mD	0.14mD	0.02 mD
Initial porosity	0.76	0.45	0.67	0.0

Task 5: Modeling of coupled flow and geomechanics in gas hydrate deposits

Subtask 5.1 Development of a coupled flow and geomechanics simulator for large deformation

This task was completed previously.

Subtask 5.2 Validation with experimental tests of depressurization

Continuing the previous work, we have still been validating T+M, finding matching parameters of geomechanics and flow, conducted in Subtask 2.1. Precisely, we are revisiting the experimental data and conditions to understand the behavior of displacement as well as to calibrate the experimental data itself.

Subtask 5.3 Modeling of sand production and plastic behavior

Continuing the previous work, we are merging the plasticity subroutines in the coupled geomechanics and gas hydrate flow code.

Subtask 5.4 Modeling of induced changes by formation of secondary hydrates: Frost-heave, strong capillarity, and induced fracturing

Continuing the previous work, we are currently coupling the fracturing simulator of ROCMECH with TOUGH+Hydrate. For preliminary study, we have successfully coupled the fracturing code of geomechanics to the single phase TOUGH+ flow simulator. Fig. 5.4.1 shows the simulation of the domain with a potential path way of fracture propagation. The injection rate is 0.5kg/s at the middle of the left side, and the reservoir permeability is 100mD. Fig. 5.4.2 shows the numerical results of fracture propagation. It shows stable fracture propagation. Also, due to leak-off to the reservoir formation, fracture propagation is delayed, compared to the case of the impermeable reservoir.

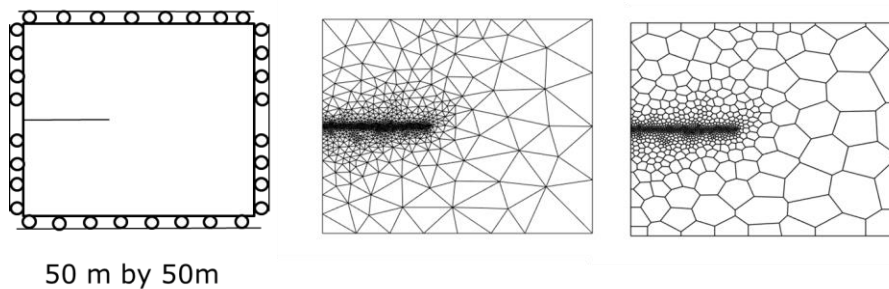


Fig. 5.4.1 Left: schematics of simulation. Right: Dual grids of geomechanics and flow, respectively.

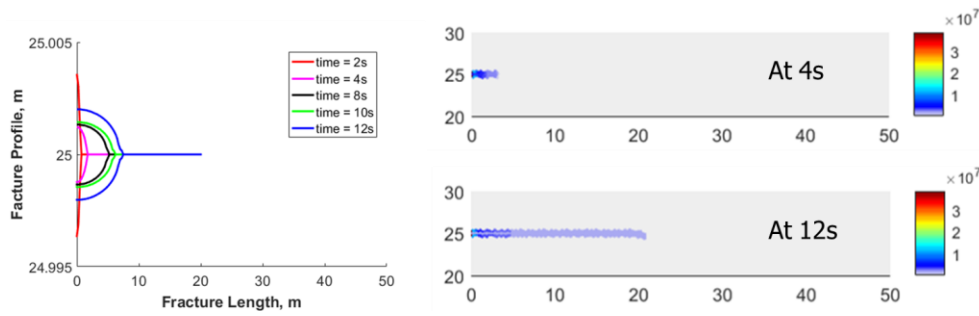


Fig. 5.4.2 Fracture propagation. Left: fracture aperture. Right: pressure distribution, where the unit is Pa.

Subtasks 5.5 and 5.6 Field-scale simulation of PBU L106 and Ulleung Basin

Continuing the previous quarter, we have been testing the field-wide simulation of two-way coupled flow and geomechanics for the UBGH2-6 site located in Ulleung Basin from the geological model made in Subtask 4.3. We have successfully performed two-way coupled simulation for long term production (i.e., 100days). For example, Fig. 5.5.1 shows distributions of pressure, gas saturation, temperature, and hydrate saturation after 100day production. Depressurization induces dissociation of gas hydrates, which can produces gas. Dissociation of gas hydrate induces temperature decreases. Fig. 5.5.2 shows substantial vertical displacement near the well and above the hydrate zone. The vertical displacement is approximately 1m after 100 days. On the other hand, the surface subsidence does not look significant. Shown in the bottom of Fig. 5.5.2, we also find that depressurization occurs mainly within the hydrate zone, not the upper (overburden) and lower (under burden) mud zones.

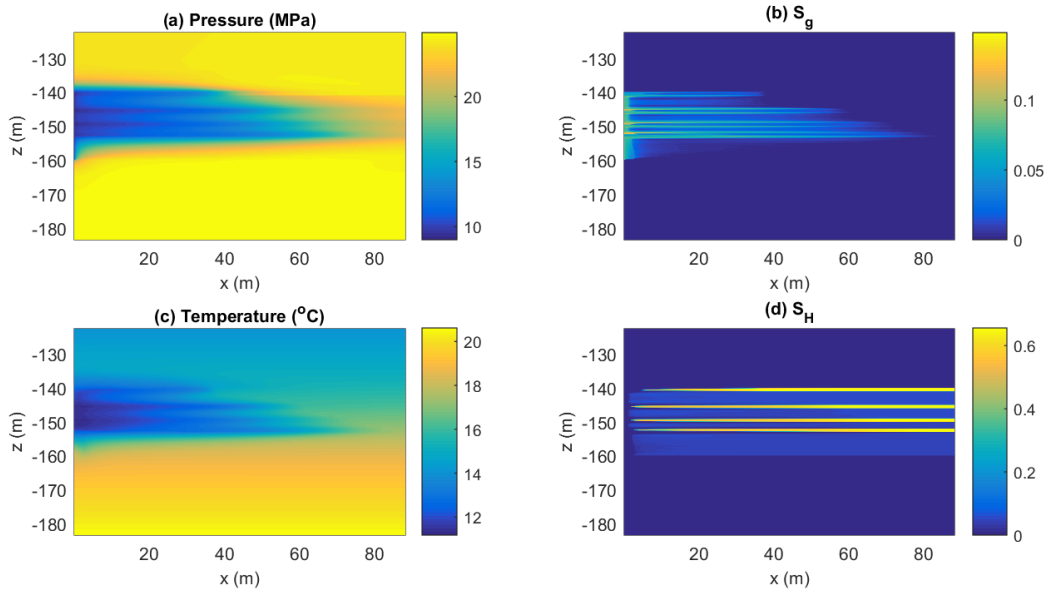


Fig. 5.5.1 Distributions of pressure (a), gas saturation (b), temperature (c), and hydrate saturation (d) after 100day production.

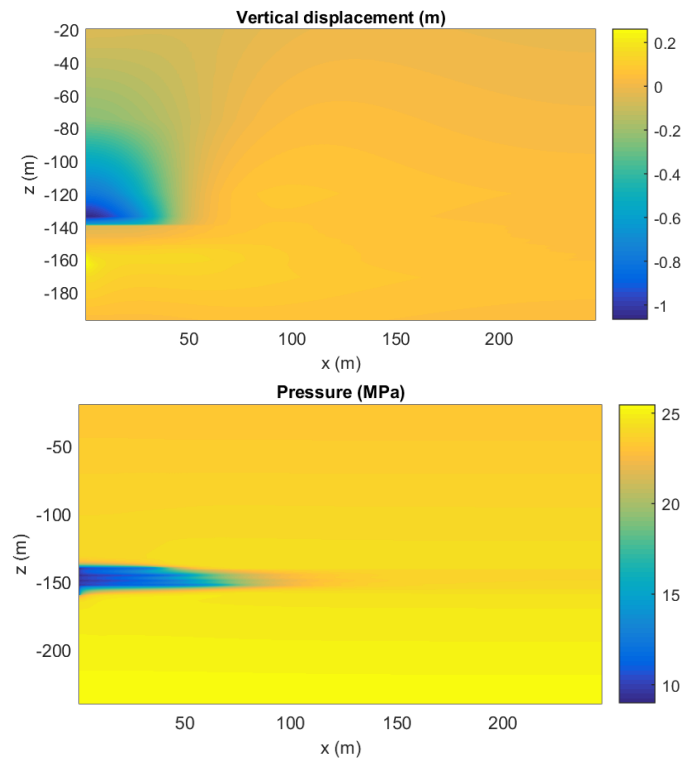


Fig. 5.5.2 Distribution of vertical displacement (top) and pressure (bottom) after 100day production.

Task 6: Simulation-Based Analysis of System Behavior at the Ignik-Sikumi and Ulleung Hydrate Deposits

No further progress was made during this quarter.

PRODUCTS

Paper submitted during this quarter

Moridis, G.J., Reagan, M.T., Queiruga, A.F., Kim, S.-J. System Response to Gas Production from a Heterogeneous Hydrate Accumulation at the UBGH2-6 Site in the Ulleung Basin of the Korean East Sea, submitted to Journal of Petroleum Sciences and Engineering

Continuing the previous activity of the web-conference, all parties of TAMU, LBNL, KIGAM have been participating in the 2nd International Gas Hydrate Code Comparison Study teleconference (IGHCCS2) held every two weeks online.

BUDGETARY INFORMATION

Table 3 shows the information of the budget for this project and the expenditure up to 09/30/2018. The expenditure by TAMU and cost-share from KIGAM are accurate while the expenditure by LBNL might not be accurate. For detailed information of the budget and expenditure, refer to the financial status report separately submitted to NETL by each institution.

Table 1 – Initial project timeline and milestones (Gantt Chart)

Quarter	FY17				FY18				FY19			
	Q1	Q2	Q3	Q4	Q1	Q2	Q3	Q4	Q1	Q2	Q3	Q4
Task 1.0. Project Management/Planning	A											
Task 2.0. Experimental study of gas hydrate in various scales for gas production of Ulleung Basin												
<i>Subtask 2.1. Depressurization of 1 m scale in 1D</i>				B								
<i>Subtask 2.2. Depressurization of 10-m scale in 1D</i>							C					
<i>Subtask 2.3. Depressurization of 1.5-m scale in 3D</i>										D		
<i>Subtask 2.4. Revisit to the centimeter-scale system</i>												
Task 3.0. Laboratory Experiments for Numerical Model Verification												

<i>Subtask 3.1. Effective stress changes during dissociation</i>				E										
<i>Subtask 3.2. Sand production</i>								F						
<i>Subtask 3.3. Secondary hydrate and capillary pressure changes</i>														G
<i>Subtask 3.4. Relative Permeability Data</i>														
<i>Subtask 3.5. Hysteresis in Hydrate Stability</i>														
Task 4.0. Incorporation of Laboratory Data into Numerical Simulation Model														
<i>Subtask 4.1. Inputs and Preliminary Scoping Calculations</i>													H	
<i>Subtask 4.2. Determination of New Constitutive Relationships</i>														
<i>Subtask 4.3. Development of Geological Model</i>														
Task 5.0. Modeling of coupled flow and geomechanics in gas hydrate deposits														
<i>Subtask 5.1 Development of a coupled flow and geomechanics simulator for large deformation</i>														I
<i>Subtask 5.2 Validation with experimental tests of depressurization</i>													J	
<i>Subtask 5.3 Modeling of sand production and plastic behavior</i>												K		
<i>Subtask 5.4 Frost-heave, strong capillarity, and induced fracturing</i>														L
<i>Subtask 5.5 Field-scale simulation of PBU L106</i>														
<i>Subtask 5.6 Field-wide simulation of Ulleung Basin</i>														
Task 6.0. Simulation-Based Analysis of System Behavior at the Ignik-Sikumi and Ulleung Hydrate Deposits														M

Table 2. Milestones Status

Milestone	Description	Planned Completion	Actual Completion	Status / Comments
Task 1 Milestones				
Milestone A	Complete the kick-off meeting and revise the PMP	12/31/17	1/14/2017	Kickoff meeting held 11/22/17, revised PMP finalized 1/17/17
Task 2 Milestones				
Milestone B	Complete analysis of 1 m-scale experiment in 1D and validation of the cm-scale system (FY17, Q4)	9/30/2017		Completed.
Milestone C	Complete analysis of 10m-scale experiment in 1D	6/30/2018		Completed.
Milestone D	Complete analysis of 1.5m-scale experiment in 3D			Completed.
Task 3 Milestones				
Milestone E	Complete geomechanical changes from effective stress changes during dissociation and construction of the relative permeability data	9/30/2017		Completed
Milestone F	Complete geomechanical changes from effective stress	9/30/2018		Completed

	changes during dissociation (sand production) and hysteresis in hydrate stability			
Milestone G	Complete geomechanical changes resulting from secondary hydrate and capillary pressure changes	9/30/2019		
Task 4 Milestones				
Milestone H	Complete inputs and preliminary scoping calculations, determination of New Constitutive Relationships, development of Geological Model	12/31/2018		
Task 5 Milestones				
Milestone I	Complete development of a coupled flow and geomechanics simulator for large deformation, validation with experimental tests of Subtasks 2.1 and 2.4.	9/30/17		Completed.
Milestone J	Validation with experimental tests of Task 2 and 3	3/31/2019		
Milestone K	Complete modeling of sand production and plastic behavior, validation with experimental tests of Subtasks 2.2	9/30/2018		
Milestone L	Complete field-scale simulation of the Ulleung Basin and PBU L106	3/31/2019		
Task 6 Milestones				
Milestone M	Complete Task 6	9/30/2019		

Table 3 Budget information

Baseline Reporting Quarter	Budget Period 1							
	Q1		Q2		Q3		Q4	
	10/01/16-12/31/16		01/01/17-03/31/17		04/01/17-06/30/17		07/01/17-09/30/17	
	Q1	Cumulative Total	Q2	Cumulative Total	Q3	Cumulative Total	Q4	Cumulative Total
Baseline Cost Plan								
Federal (TAMU)	\$37,901	\$37,901	\$57,809	\$95,711	\$43,967	\$139,678	\$34,206	\$173,884
Federal (LBNL)	\$18,750	\$18,750	\$18,750	\$37,500	\$18,750	\$56,250	\$18,750	\$75,000
Non-Federal Cost Share	\$6,986	\$6,986	\$6,986	\$13,972	\$6,986	\$20,958	\$656,986	\$677,944
Total Planned	\$63,637	\$63,637	\$83,545	\$147,183	\$69,703	\$216,886	\$709,942	\$926,828
Actual Incurred Cost								
Federal (TAMU)	\$0	\$0	\$10,235	\$10,235	\$57,085	\$67,321	\$54,167	\$121,488
Federal (LBNL)	\$0	\$0	\$0	\$0	\$0	\$0	\$8,500	\$8,500
Non-Federal Cost Share	\$0	\$0	\$6,986	\$6,986	\$6,986	\$13,972	\$156,986	\$170,958
Total incurred cost	\$0	\$0	\$17,221	\$17,221	\$64,071	\$81,293	\$219,653	\$300,946
Variance								
Federal (TAMU)	(\$37,901)	(\$37,901)	(\$47,574)	(\$85,475)	\$13,118	(\$72,357)	\$19,961	(\$52,396)
Federal (LBNL)	(\$18,750)	(\$18,750)	(\$18,750)	(\$37,500)	(\$18,750)	(\$56,250)	(\$10,250)	(\$66,500)
Non-Federal Cost Share	(\$6,986)	(\$6,986)	\$0	(\$6,986)	\$0	(\$6,986)	(\$500,000)	(\$506,986)
Total variance	(\$63,637)	(\$63,637)	(\$66,324)	(\$129,961)	(\$5,632)	(\$135,593)	(\$490,289)	(\$625,882)

Baseline Reporting Quarter	Budget Period 2							
	Q1		Q2		Q3		Q4	
	10/01/17-12/31/17		01/01/18-03/31/18		04/01/18-06/30/18		07/01/18-09/30/18	
	Q1	Cumulative Total	Q2	Cumulative Total	Q3	Cumulative Total	Q4	Cumulative Total
Baseline Cost Plan								
Federal (TAMU)	\$42,481	\$42,481	\$35,307	\$77,788	\$46,367	\$124,155	\$39,908	\$164,063
Federal (LBNL)	\$18,750	\$18,750	\$18,750	\$37,500	\$18,750	\$56,250	\$18,750	\$75,000
Non-Federal Cost Share	\$6,986	\$6,986	\$6,986	\$13,972	\$6,986	\$20,958	\$6,986	\$27,944
Total Planned	\$68,217	\$68,217	\$61,043	\$129,260	\$72,103	\$201,363	\$65,644	\$267,007
Actual Incurred Cost								
Federal (TAMU)	\$35,832	\$35,832	\$31,662	\$67,494	\$35,510	\$103,004	\$86,971	\$189,974
Federal (LBNL)	\$45,952	\$45,952	\$18,130	\$64,082	\$0	\$64,082	\$4,990	\$69,072
Non-Federal Cost Share	\$6,986	\$6,986	\$6,986	\$13,972	\$506,986	\$520,958	\$6,986	\$527,944
Total incurred cost	\$88,770	\$88,770	\$56,778	\$145,548	\$542,496	\$688,044	\$98,947	\$786,990
Variance								
Federal (TAMU)	(\$6,650)	(\$6,650)	(\$3,645)	(\$10,294)	(\$10,857)	(\$21,151)	\$47,062	\$25,911
Federal (LBNL)	\$27,202	\$27,202	(\$620)	\$26,582	(\$18,750)	\$7,832	(\$13,760)	(\$5,928)
Non-Federal Cost Share	\$0	\$0	\$0	\$0	\$500,000	\$500,000	\$0	\$500,000
Total variance	\$20,552	\$20,552	(\$4,265)	\$16,288	\$470,393	\$486,681	\$33,302	\$519,983

Baseline Reporting Quarter	Budget Period 3							
	Q1		Q2		Q3		Q4	
	10/01/18-12/31/18		01/01/19-03/31/19		04/01/19-06/30/19		07/01/19-09/30/19	
	Q1	Cumulative Total	Q2	Cumulative Total	Q3	Cumulative Total	Q4	Cumulative Total
Baseline Cost Plan								
Federal (TAMU)	\$43,543	\$43,543	\$36,189	\$79,733	\$47,526	\$127,259	\$41,209	\$168,468
Federal (LBNL)	\$18,750	\$18,750	\$18,750	\$37,500	\$18,750	\$56,250	\$18,750	\$75,000
Non-Federal Cost Share	\$6,986	\$6,986	\$6,986	\$13,972	\$6,986	\$20,958	\$6,986	\$27,944
Total Planned	\$69,279	\$69,279	\$61,925	\$131,205	\$73,262	\$204,467	\$66,945	\$271,412
Actual Incurred Cost								
Federal (TAMU)								
Federal (LBNL)								
Non-Federal Cost Share								
Total incurred cost								
Variance								
Federal (TAMU)								
Federal (LBNL)								
Non-Federal Cost Share								
Total variance								

National Energy Technology Laboratory

626 Cochrans Mill Road
P.O. Box 10940
Pittsburgh, PA 15236-0940

3610 Collins Ferry Road
P.O. Box 880
Morgantown, WV 26507-0880

13131 Dairy Ashford Road, Suite 225
Sugar Land, TX 77478

1450 Queen Avenue SW
Albany, OR 97321-2198

Arctic Energy Office
420 L Street, Suite 305
Anchorage, AK 99501

Visit the NETL website at:
www.netl.doe.gov

Customer Service Line:
1-800-553-7681



U.S. DEPARTMENT OF
ENERGY

**NATIONAL ENERGY
TECHNOLOGY LABORATORY**